Method for the Study of Gaseous Oxidants for the Oxidation of Mercury Gas

ARTICLE *in* INDUSTRIAL & ENGINEERING CHEMISTRY RESEARCH · JUNE 2005

Impact Factor: 2.59 · DOI: 10.1021/ie050377j

3 AUTHORS, INCLUDING:

Shou-Heng Liu
National Kaohsiung University of Applied Sci…
35 PUBLICATIONS **566** CITATIONS
SEE PROFILE

Shih-Ger Chang
Lawrence Berkeley National Laboratory
73 PUBLICATIONS **821** CITATIONS
SEE PROFILE

Method for the Study of Gaseous Oxidants for the Oxidation of Mercury Gas

Nai-Qiang Yan,[†] Shou-Heng Liu,[‡] and Shih-Ger Chang*

Environmental Energy Technology Division, Lawrence Berkeley National Laboratory, University of California, Berkeley, California 94720

Charles Miller

National Energy Technology Laboratory, Pittsburgh/Morgantown, Pennsylvania 15236/West Virginia 26507

The oxidation rate constants of mercury gas (Hg^0) are difficult to determine because Hg^0 easily adsorbs on reactor walls and the reactions can be catalyzed by the solid surface. Also, the UV light which is commonly used to monitor the Hg^0 concentration can accelerate the reaction. We have demonstrated a procedure that allows the determination of gas-phase, surface-catalyzed, and photoinduced contributions in the kinetic study of the reaction of Hg^0 with chlorine gas. By experimenting with several reactors having different surface-to-volume ratios, the relative contributions of gas-phase and surface-catalyzed reactions were determined. The pressure-dependent study revealed that the gas-phase oxidation was by means of a three-body collision process. The third-order rate constant was determined to be 7.5 ($\pm$0.2) $\times$ 10^{-39} cm^6·$molecules^{-2}$·s^{-1} with N_2 as the third body at 297 $\pm$ 1 °K. The surface catalyzed reaction on a quartz window was second order, and the rate constant was 2.7 $\times$ 10^{-17} mL^2·$molecules^{-1}$·cm^{-2} sec. The photoinduced contribution was obtained by comparing the Hg^0 decay rate between continuous and intermittent irradiations. The utilization efficiency of 253.7 nm photons for Hg^0 oxidations at a chlorine concentration of 6.5 $\times$ 10^{15} molecules·mL^{-1} was $<$6.7 $\times$ 10^{-4} molecules·$photon^{-1}$.

Introduction

Among human activities, coal-fired power plants represent a primary mercury emission source. Although the levels of mercury in coal are small (0.04−0.53 mg·kg^{-1}),[1,2] the amount of coal burned is huge. Indications are that a majority of the mercury in coal is converted to the elemental form (Hg^0) in the high-temperature combustion zone and that the oxidation may occur as the combustion gases cool.[3−5] The amount of Hg^0 oxidized depends very much on the type of coal burned.[3,6] The amount of Hg^0 oxidized also depends on the type of air pollution control devices installed on the unit and the operating conditions at which the unit is operated.[7] Hg^0 is most difficult to capture because it is volatile and insoluble in water. If it is released to the atmosphere, it can remain aloft for months, spreading over vast regions of the globe.[8]

Unlike Hg^0, the oxidized mercury in the form of mercuric or mercurous salts is much less volatile and more soluble in water. As a result, it can be more easily captured by existing coal utility pollution control equipment, such as baghouse/ESP (electrostatic precipitator) or wet SO_2 scrubbers.[9−12] In this context, a cost-effective approach for the control of mercury emissions could be developed, if an oxidant can be identified for injection into the duct downstream (air preheater, ESP, or baghouse) of a coal-fired power plant system to oxidize the Hg^0 selectively and rapidly. The kinetics of the oxidation of Hg^0 by gas oxidants under flue gas conditions has not been well-studied. Although many gas-phase reactions involving Hg^0 have been studied,[3,6,13−21] several of them reported the upper limit of rate constants.[13−15] This is because the gas-phase oxidation of Hg^0 is difficult to study because the Hg^0 easily adsorbs on solid surface and its reactions can be catalyzed by the surface.[16−18] Consequently, any analytical instrument for Hg^0 determination could produce erroneous results if it requires the transfer of samples. Also, the 253.7 nm photons, which are used to monitor the Hg^0 concentration, can accelerate the reactions, as will be demonstrated in this study.

In this paper, various types of experiments were performed to determine, for the first time in the kinetic study of Hg^0 reactions, the relative contributions of each of three concurrent mechanisms in the oxidation of Hg^0 by Cl_2. The three concurrent mechanisms include the gas-phase, reactor-surface-catalyzed, and photoinduced oxidations of Hg^0 by Cl_2. The effect of flue gas constituents, such as SO_2, NO_x, CO, and fly ash, on the reaction of Hg^0 with Cl_2 will be reported in a separate paper.

Experimental Section

Apparatus. The apparatus (Figure 1) used for kinetic studies includes a self-assembled cold vapor atomic absorption spectrophotometer (CVAAS), a glass reactor (Pyrex), and a vacuum system for gas handling. A low-pressure mercury lamp (Oriel, model 6035) was used as the 253.7 nm UV light source. The light beam was collimated with a lens before passing the reactor through the quartz windows. After passing the reactor, the light

* To whom correspondence should be addressed. Tel.: (510) 486-5125. Fax: (510) 486-7303. E-mail: sgchang@lbl.gov.

[†] On leave from the School of Environmental Science and Engineering, Shanghai Jiao Tong University, People's Republic of China.

[‡] On leave from Environmental Engineering Department, Taiwan Cheng-Kung University, Tainan, Taiwan, Republic of China.

10.1021/ie050377j CCC: $30.25
Published on Web 06/23/2005

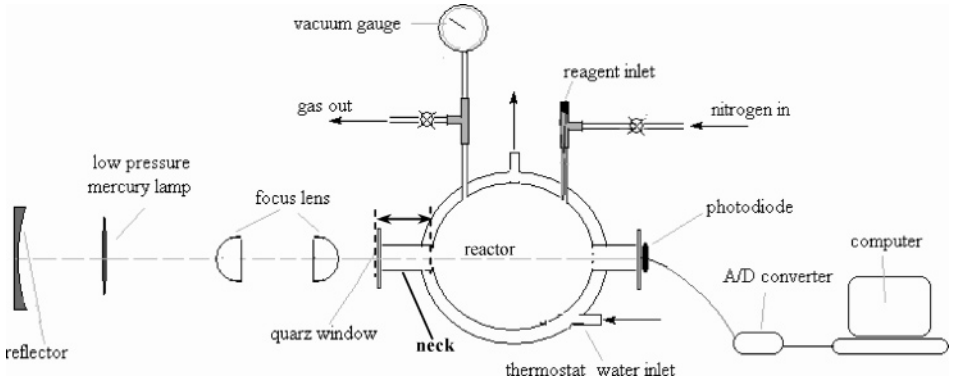

Figure 1. Schematic diagram of the experimental system.

was detected by a photodiode (Edmund, model NT54-037). The intensity data as a function of time was recorded in a computer via an A/D converter (DataQ, model DI-700). The concentration of Hg^0 in the reactor was measured in situ, with the capability of a time resolution of 20 milliseconds.

The Pyrex reactors used for the kinetic study were spherical and oval shapes with two short necks (diam 20.5 mm and length 18 mm) connected for attaching quartz windows. Three sizes of reactors with different surface-to-volume ratios were employed for determining the contribution of the surface and photoinduced reactions. The volumes of the three reactors were 190, 380, and 960 mL, with a surface area of 190, 255, and 498 cm^2, respectively, corresponding to the ratio of the volume-to-surface area of 1, 1.49, and 1.93 $mL \cdot cm^{-2}$. (In this paper, the unit of the volume and gas concentration is expressed in mL and molecules/mL, respectively, to avoid canceling with the surface unit, cm^2.) The surface areas of the quartz windows and the optical path, which were identical for all three reactors, were 6.6 cm^2 and 14.5 cm, respectively. The reactors could be readily exchanged from one to another in the assembly. The reactor was cleaned with deionized water frequently to minimize the effect of the product on the wall. All the inner walls of the Teflon gas tubes and valves connected to the reactors were coated with halocarbon wax (HW) to minimize the Hg^0 adsorption.

The light intensity was measured by a thermopile (Eppley, serial no. 16034E6) and the chemical actinometry method employing potassium ferrioxalate.[22] The average intensity measured at the reactor was 6.06×10^{16} photons$\cdot cm^{-2} \cdot s^{-1}$, and this was in good agreement between both methods.

Chemicals. The chlorine (calibrated standard gas of 5000 ppm with N_2 making up the balance) and nitrogen (high purity grade) were from Airgas Co. Halocarbon wax (HW, series 1500) was from Halocarbon Product Co. Mercury (99.99%), H_2SO_4 (98%), $K_2C_2O_4$ (99%), $FeCl_3 \cdot 6H_2O$ (98%), $FeSO_4 \cdot 7H_2O$ (99%), and 1,10-phenanthroline (95%) were from Sigma-Aldrich.

Procedures. The kinetics was performed using the absolute rate technique under pseudo-first-order conditions[23] with respect to Hg^0. The Hg^0 and Cl_2 were introduced into the reactor by injection with a syringe. Initially, the reactor was evacuated, and then a volume of nitrogen gas saturated with Hg^0 was injected with a syringe (B-D Yale, 100 mL) to the reactor to reach a pressure of about 250 Torr (1 atm = 760 Torr). The pressure in the reactor was then brought up to 500 Torr with nitrogen gas. Subsequently, a volume of a known concentration of Cl_2 in nitrogen was injected by a syringe into the reactor before the pressure was quickly brought to 760 Torr with nitrogen. The concentration of Cl_2 was measured at 330 nm with a UV-visible spectrophotometer (Perkin-Elmer, Lambda-02). Nitrogen instead of air was used as the balance gas to avoid the mercury-photosensitized reaction because of oxygen.[9,21] The reactor was cleaned with deionized water after each run to minimize the possible effect of the products deposited on the wall from the previous run.

The rate of disappearance of Hg^0 in the reactors was monitored at 253.7 nm by CVAAS during the course of the reaction. However, the loss of Hg^0 in the reactor as measured by the CVAAS could come from several reaction pathways: (1) adsorption on the reactor wall and quartz window, (2) gas-phase reaction, (3) surface-induced reaction, and (4) photoinduced reaction. The adsorption of Hg^0 on the wall was investigated by performing an experiment without chlorine while monitoring the concentration decay of the Hg^0 in the reactor as a function of time.

The adsorption can be minimized by coating the wall with HW. However, the quartz windows cannot be coated with HW because it attenuates the light (253.7 nm). To determine the Hg^0 loss from the adsorption on the windows, experiments were performed with three reactors having different ratios of window surface area to the reactor volume.

The effect of light on the reaction rate was studied by comparing the Hg^0 decay rate between a continuous irradiation and intermittent irradiation. In the intermittent irradiation, the light was shielded from entering the reactor most of the time until a reading of the Hg^0 concentration was taken. The shielding was taken off only a few seconds and then immediately put back on. This process occurred periodically. The results from these two sets of experiments on three reactors allowed the determination of the relative contributions of the gas-phase, photoinduced gas-phase, window-surface-induced, and photoinduced surface reactions.

The uncertainty of the Hg^0 concentrations measured by CVAAS under the experimental conditions employed was ± 0.005 ppm. The uncertainty of the concentration of Cl_2 could be controlled to within ± 0.5 ppm. The accuracy of the reaction rate constants determined from the gas concentration measurements and the fluctuation of the experimental data was within 20%.

Result and Discussion

Adsorption on the Wall. The adsorption of Hg^0 on the wall was investigated, without Cl_2 in three reactors at 297 ± 1 K. Figure 2 shows that the rate of the

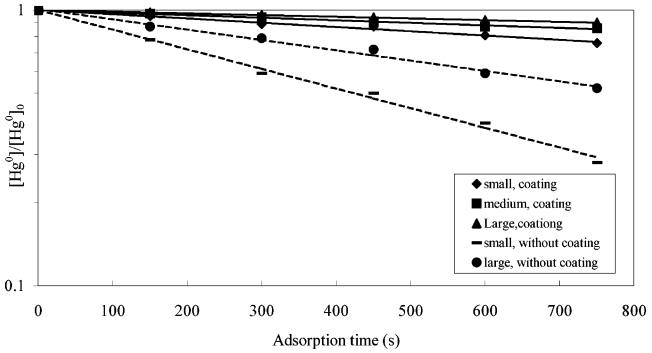

Figure 2. Semilogarithmic plots of changes of the relative Hg^0 concentrations, due to the adsorption of Hg^0 on the reactor surface, over time at 297 ± 1 K. Three reactor sizes were studied: a small reactor with 190 mL volume and 190 cm^2 surface area, a medium reactor with 380 mL and 255 cm^2, and a large reactor with 960 mL and 498 cm^2. The effect of the surface coating by the halocarbon wax was studied. The initial mercury concentration, $[Hg^0]_0$, employed was 4.4×10^{12} molecules·mL^{-1}.

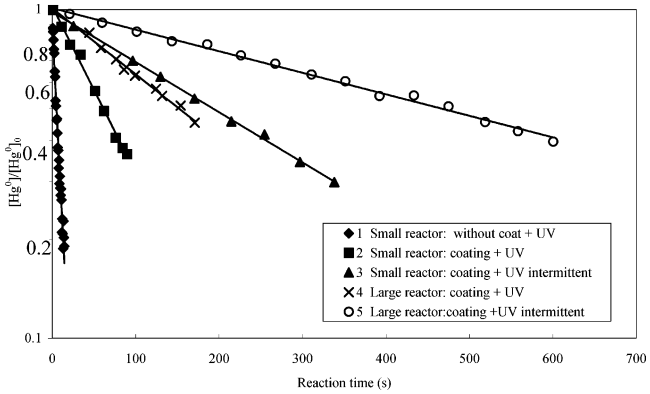

Figure 3. Overall Hg^0 depletion rates in the presence of Cl_2 at various conditions at 297 K. It plots the semilogarithmic changes of the relative Hg^0 concentrations over time. The effect of reactor sizes, surface coating, and UV irradiation on the Hg^0 depletion rates was shown. The initial concentrations of Hg^0 and Cl_2 were 4.4×10^{12} molecules·mL^{-1} and 6.5×10^{15} molecules·mL^{-1}, respectively.

adsorption of Hg^0 on the wall (Pyrex) without coating was very significant. The Hg^0 initial concentration, $[Hg^0]_0$, was 0.18 ppm (1 ppm = 2.46×10^{13} molecules·mL^{-1} at 297 K). After 300 s, ~41% and 20% of Hg^0 originally in the gas phase had adsorbed on the wall of the small and large reactor, respectively. The adsorption rate decreased substantially if the wall had been coated with HW. Only 11%, 7%, and 4% of Hg^0 had adsorbed on the wall in the small, medium, and large reactors, respectively, after 300 s.

Additionally, it was observed that the adsorption rate of Hg^0 displayed an exponential decay curve, which can be described by the following first-order kinetic equation

$$\Sigma A_a R_a = (A_q k_{aq} + A_w k_{aw})[Hg^0] \quad (1)$$

where R_a (molecules·cm^{-2}·s^{-1}) is the Hg^0 adsorption rate, k_{aq} and k_{aw} ($mL \cdot cm^{-2} \cdot s^{-1}$) represent the adsorption rate constant on quartz and halocarbon wax coated wall surfaces, respectively. A_a is either A_q or A_w; A_q and A_w are the areas of the quartz windows and the HW-coated reactor wall, respectively. $A_w k_{aw}$ should be replaced by $A_p k_{ap}$ if the Pyrex wall was not coated with HW. By measuring the rate of the disappearance of Hg^0 in three reactors, the adsorption rate constants were calculated to be 1.4×10^{-3}, 1.7×10^{-3}, and 2.5×10^{-4} $mL \cdot cm^{-2} \cdot s^{-1}$ for the quartz, Pyrex, and HW-coated wall surfaces, respectively. The Hg^0 adsorption rate constant on the HW-coated wall is almost an order of magnitude smaller than that on the wall without the coating.

Whether the adsorbed Hg^0 on the quartz window will attenuate the light intensity (253.7 nm photons) and interfere with the kinetic study of Hg^0 with Cl_2 was assessed. The Hg^0 concentration employed was 4.4×10^{12} molecules·mL^{-1} (0.18 ppm). The total number of Hg^0 molecules initially introduced into the small (190 mL), medium (380 mL), and large (960 mL) reactors was 9.2×10^{14}, 1.84×10^{15}, and 4.65×10^{15} molecules, respectively. From the adsorption rate constant on the quartz window, the number of Hg^0 molecules adsorbed on the quartz window was calculated to be 7.05×10^{12} molecules after 300 s, which was the time period when most of the kinetic data were collected. Therefore, $<1/100$th of the Hg^0 initially introduced was adsorbed on the quartz window during the course of the reaction. Also, the number of Hg^0 molecules required to cover one monolayer on the quartz window (6.6 cm^2) was estimated to be 9.34×10^{15} molecules. Therefore, the Hg^0 adsorbed on the window in 300 s was $<1/1000$th of a monolayer. When using the absorption cross-section of Hg^0, $\sigma = 4.5 \times 10^{-16}$ cm^2·$molecules^{-1}$ at 253.7 nm,[25] and assuming $1/1000$th of a monolayer of Hg^0 adsorbed on the quartz surface, the light attenuated by the adsorbed Hg^0 is only 0.05%, which is negligible in this kinetic study.

The effect of pressure on the Hg^0 adsorption rate was studied. We found that the adsorption rate is proportional to the total gas pressure in the reactor. With the same initial Hg^0 concentration of 4.4×10^{12} molecules·mL^{-1}, by reducing the gas pressure from 1 atm to 245 Torr, the loss of Hg^0 in the gas phase decreased to ~4% and 1% after 300 s in the small and large reactors, respectively.

The Overall Hg^0 Depletion Rate. The typical depletion curves of Hg^0 in the presence of Cl_2 under various experimental conditions were depicted in Figure 3. The initial concentrations of Hg^0 and Cl_2 in all the runs were 4.4×10^{12} and 6.5×10^{15} molecules·mL^{-1}, respectively, with the balance N_2 gas to 1 atm. Experiments were performed at 297 ± 1 K. The Hg^0 depletion rate was rather rapid when the reactor wall was not coated with the HW (compare curves 1 and 2, given the same small reactor), which suggests that, in addition to the much slower adsorption rate (Figure 2), the Pyrex wall catalyzed the reaction of Hg^0 with Cl_2. The presence of the photoinduced reaction is obvious from the fact that the Hg^0 depletion rate is faster in runs under the continuous (curve 4) rather than the intermittent (curve 5) irradiation.

Even under the conditions where the Pyrex reactor wall was coated with HW and the reactions proceeded in the dark, the depletion rate of Hg^0 was faster in the small reactor (curve 3) than in the larger one (curve 5). This result indicates that the surface of the quartz window and the reactor wall after coating the HW should still contribute to the depletion of Hg^0. The magnitude of the Hg^0 depletion from reactions on the quartz window, on the HW-coated reactor wall, and in the gas phase can be calculated by conducting experiments in three reactors with different surface-to-volume ratios as discussed before.

The depletion of Hg^0 under all experimental conditions follows a first-order reaction rate law[22] with respect to Hg^0, as can be seen when plotting the

logarithm of the relative Hg^0 concentration over the reaction time (Figure 3). Thus, the overall depletion rate of Hg^0 can be expressed by eq 2

$$-\mathrm{d}[Hg^0]/\mathrm{d}t = k_T[Hg^0] \quad (2)$$

where k_T is the apparent overall depletion rate constant in s^{-1}. $[Hg^0]$ is the concentration of Hg^0 in the gas phase in molecules·mL^{-1}.

The fact that the overall Hg^0 depletion rate follows a first-order rate equation can be used to suggest that individual Hg^0 depletion pathways involved also follow a first-order rate equation. This suggestion is based on the employment of the following experimental observations and conditions. When the experiment was conducted in a reactor with an HW coating and in the dark (e.g., curves 3 and 5), the overall Hg^0 depletion in the reactor constitutes three pathways: the gas-phase reaction, the adsorption, and the reaction on the surface. The gas-phase reaction of Hg^0 with Cl_2 can be regarded as the pseudo-first-order reaction with respect to Hg^0, because the concentration of Cl_2 was much larger than that of Hg^0. The adsorption rate was proportional to the Hg^0 concentration, as demonstrated (eq 1). Consequently, the remaining surface reaction pathway must follow the first-order rate law, given the fact that its contribution to the total Hg^0 depletion is very significant. Likewise, the photoinduced reaction and the reaction on the Pyrex surface can be considered as the first-order reaction from curves 1, 2, and 4 in Figure 3.

On the basis of the aforementioned analysis, the overall rate of the disappearance of Hg^0 (eq 2) can be further expressed with eq 2a, in which the surface adsorption is combined with the surface reaction as it will be treated as one pathway in depleting the Hg^0 from the gas phase, as follows

$$-\mathrm{d}[Hg^0]/\mathrm{d}t = [k_g' + k_p'(V_p/V) + \alpha_q(k_{aq} + k_{sq}')A_q/V + \alpha_w(k_{aw} + k_{sw}')A_w/V]\,[Hg^0] \quad (2a)$$

where V_p is the volume of gas in the reaction that was illuminated by the light and V is the total volume of the reactor. k_g' and k_p' represent the pseudo-first-order rate constants of the gas-phase and photoinduced reactions, s^{-1}; k_{sq}' and k_{sw}' are the pseudo-first-order rate constants of surface reactions on the quartz and the halocarbon-wax-coated surface, mL·s^{-1}·cm^{-2}.

A_q and A_w are the surface area of the quartz window and the inner wall of the reactor, cm^2, respectively. α_q or α_w is equal to $[Hg^0]_s/[Hg^0]$, which is a concentration distribution coefficient (≤ 1) between the local gas-phase Hg^0 concentration adjacent to the surface, $[Hg^0]_s$, and the bulk gas-phase Hg^0 concentration (further discussion in eq 8).

On the basis of eqs 1 and 2a, the overall rate constant, k_T, can be expressed as follows.

$$k_T = k_g' + (V_p/V)k_p' + \alpha_q(k_{aq} + k_{sq}')A_q/V + \alpha_w(k_{aw} + k_{sw}')A_w/V \quad (3)$$

k_T was obtained directly from the experiment. However, a series of experiments must be performed to determine the contributions of each reaction pathway and to evaluate the corresponding rate constants.

Gas-Phase Reaction Rate. To minimize the photoinduced reaction, the light was allowed to pass through the reactor for the Hg^0 measurement about 2 s for every 40−60 s of reaction. Thus, the effect of UV was trifling, and the second term in eq 3 can be neglected ($V_p = 0$). The wall of the reactor, except the quartz windows, was coated with HW . Thus, eq 3 can be reduced to

$$k_T = k_g' + \alpha_q(k_{aq} + k_{sq}')A_q/V + \alpha_w(k_{aw} + k_{sw}')A_w/V \quad (4)$$

where the subscripts sq and sw represent the surface of the quartz windows and the HW-coated reactor wall, respectively. The three terms on the right of eq 4 represent the contribution of the gas-phase reaction, the quartz surface, and the HW-coated reactor wall, respectively.

The terms k_g', $\alpha_q(k_{aq} + k_{sq}')$, and $\alpha_w(k_{aw} + k_{sw}')$ in eq 4 can be calculated from k_T by performing reactions in three reactors with different surface-to-volume ratios; the results are shown in Table 1.

The calculated value of $\alpha_q(k_{aq} + k_{sq}')$ for the quartz surface was much larger than the adsorption rate constant k_{aq} ($\sim 1.4 \times 10^{-3}$ mL·cm^{-2}·s^{-1} as indicated before), implying that the surface reaction rate was more rapid than the adsorption rate. Consequently, the adsorption on the quartz surface was neglected, and $\alpha_q k_{sq}'$ was used in Table 1 instead of $\alpha_q(k_{aq} + k_{sq}')$.

On the contrary, the value of $\alpha_w(k_{aw} + k_{sw}')$ for the HW-coated surface (Table 1) was almost the same as the adsorption rate constant k_{aw} (0.25×10^{-3} mL·cm^{-2}·s^{-1}), suggesting that the surface reaction on the HW-coated surface was slow. Therefore, the contribution of the surface reaction on the HW-coated reactor wall was neglected.

Meanwhile, the results (Table 1) show that the contribution of the gas-phase reaction to the overall reaction, k_g'/k_T, was smaller in the small reactor than in the larger one, as should be expected. For example, the percentage of the pseudo-first-order gas-phase rate constant to the overall rate constant, k_g'/k_T was determined to be 21.0%, 34.4%, and 58.7% for reactors with 190 mL, 380 mL, and 960 mL volume, respectively, at a Cl_2 concentration of 2.5×10^{15} molecules·mL^{-1} (Table 1).

Also, the relative contribution of the gas-phase reaction increases with an increase of the Cl_2 concentration (Table 1), given the same reactor. For example in the 960 mL reactor, k_g'/k_T was 50.5%, 58.7%, and 71.1% with $[Cl_2]$ of 1.3×10^{15}, 2.5×10^{15}, and 6.5×10^{15} molecules·mL^{-1}, respectively. This is because the surface reaction rate is determined by both the chemical reaction rate on the surface and the Hg^0 diffusion rate from the bulk to the surface. A detailed discussion and mathematical equation (eq 10) will be presented later.

Additionally, k_g' was proportional to the concentration of Cl_2 (Table 1), which indicates that the gas-phase reaction rate is overall second order, being first order with respect to both Hg^0 and Cl_2. The gas-phase reaction rate constants of Hg^0 with Cl_2 determined from various conditions in three reactors were in very good agreement and averaged to be 1.82×10^{-19} mL·molecules^{-1}·s^{-1} at 1 atm and 297 ± 1 K.

The effect of gas pressure on the overall reaction rate was studied. Figure 4 shows the overall pseudo-first-order rate constant,[22] k_T, as a function of pressure and reactor size, with intermittent (solid line) and continuous (dotted line) UV radiation. The Hg^0 and Cl_2 concentrations in all the runs were 4.4×10^{12} and 6.5×10^{15} molecules·mL^{-1}, respectively. The balance of the

Table 1. Calculated Results of k_g', $\alpha_q k_{sq}'$, and $\alpha_w(k_A + k_{sw}')$[a] for Gas-Phase and Surface-Reaction Pathways of Hg^0 with Cl_2 from Three Reactors with Various $[Cl_2]$ at 1 atm

$[Cl_2]$ (molecules·mL^{-1})	V (mL)	k_g' ($\times 10^{-3}$ s^{-1})	$\alpha_q k_{sq}'$[b] ($\times 10^{-3}$ mL·cm^{-2}·s^{-1})	$\alpha_w(k_{aw} + k_{sw}')$ ($\times 10^{-3}$ mL·cm^{-2}·s^{-1})	k_g'/k_T[c] (%)	$k_g'/[Cl_2]$ ($\times 10^{-19}$ mL·molecules^{-1}·s^{-1})
6.5×10^{15}	190	1.2 ± 0.05	49.1 ± 1.0	0.28 ± 0.02	33.1%	1.85 ± 0.05
	380				51.3%	
	960				71.1%	
2.5×10^{15}	190	0.46 ± 0.03	33.5 ± 1.0	0.28 ± 0.01	21.0%	1.80 ± 0.05
	380				34.4%	
	960				58.7%	
1.3×10^{15}	190	0.24 ± 0.03	22.5 ± 1.0	0.27 ± 0.01	17.1%	1.82 ± 0.05
	380				26.6%	
	960				50.5%	

[a] k_g', k_{sq}', and k_{sw}' represent the pseudo-first-order rate constants of the gas-phase reaction, the surface reaction on the quartz, and the halocarbon-wax-coated wall, respectively. [b] $\alpha_q k_{aq}$ was neglected because it was much smaller than $\alpha_q k_{sq}'$. [c] k_g'/k_T is the ratio of the contribution of the gas-phase reaction to the overall reaction.

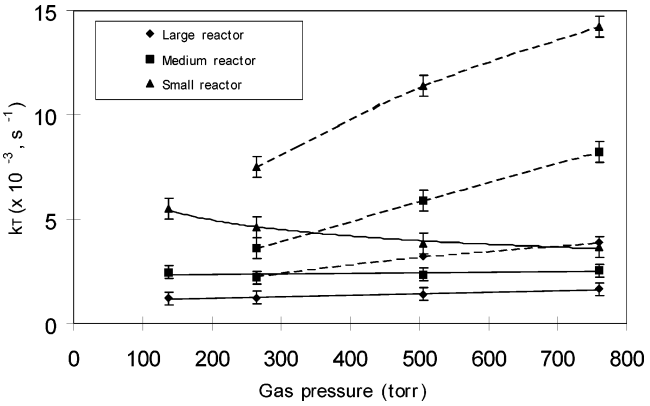

Figure 4. Overall rate constants as a function of the gas pressure from 120 Torr to 770 Torr in three sizes of reactors. The initial Hg^0 and Cl_2 concentrations were 4.4×10^{12} molecules·mL^{-1} and 6.5×10^{15} molecules·mL^{-1}, respectively. All the reactors were coated with halocarbon wax. Solid lines indicate conditions without UV, while dotted lines indicate conditions with UV.

gas in the reactor was nitrogen. It can be seen that the k_T increased with the decrease of the pressure in the small reactor. On the contrary, k_T decreased with the decrease of the gas pressure in the large reactor. This behavior can be explained as follow: The small reactor has a larger surface component because it has a larger surface-to-volume ratio compared to that of the larger reactor. The surface reaction on the quartz is more favorable at a reduced pressure due to the increase of the diffusion coefficient, which is inversely proportional to the gas pressure.[24] However, the gas-phase reaction rate would decrease with the decrease of the pressure if it goes through a third body collision process. In other words, there are two reaction mechanisms taking place simultaneously: an increase with a decrease of the total pressure and a decrease with a decrease of the pressure. Figure 4 shows the effect of the pressure on the pseudo-first-order overall rate constant, i.e., the sum of the two reaction mechanisms, in three reactors. Therefore, the overall rate constant should increase with the decrease of the pressure if the surface reaction is dominant, such as the case of a small reactor.

Similarly, by performing experiments in three reactors under different gas pressure, k_g' and $\alpha_q k_{sq}'$ were calculated (Table 2) from the k_T values obtained experimentally. It was obvious that the apparent surface reaction rate constant, $\alpha_q k_{sq}'$, on the quartz increased with the decrease of the gas pressure. Whereas, the pseudo-first-order[22] gas-phase rate constant k_g' showed a linear dependence on the gas pressure. This implies that the gas-phase reaction of Hg^0 and Cl_2 can be

Table 2. Effect of Gas Pressure on k_g' and $\alpha_q k_{sq}'$ for the Gas-Phase and Surface-Reaction Pathways of Hg^0 with Cl_2 at 297 ± 1 K[a]

gas pressure (Torr)	V (mL)	k_g' ($\times 10^{-3}$ s^{-1})	$\alpha_q k_{sq}'$ ($\times 10^{-3}$ mL·cm^{-2}·s^{-1})	k_g'/k_T (%)	$k_g'/[Cl_2]$ ($\times 10^{-19}$ mL·molecules^{-1}·s^{-1})
506	190	0.8 ± 0.05	64.2	22.8%	1.20 ± 0.1
	380			35.3%	
	960			64.3%	
264	190	0.43 ± 0.03	88.5	10.9%	0.66 ± 0.08
	380			21.1%	
	960			39.2%	

[a] $[Cl_2]$ at 6.5×10^{15} molecules·cm^{-3}.

regarded as a three-body collision reaction

$$Hg^0 + Cl_2 + M \rightarrow HgCl_2 + M \quad (5)$$

$$R_g = k_g'[Hg^0] = k_g[Cl_2][Hg^0] = k_3[M][Cl_2][Hg^0] \quad (6)$$

where M represents the third body, which is N_2 in this case. The third-order gas-phase reaction rate constant, k_3, was determined to be 7.5 (±0.2) $\times 10^{-39}$ cm^6·molecules^{-2}·s^{-1} at 297 ± 1 K. Thus, the second-order reaction rate constant of Hg^0 with Cl_2, k_g, is 1.82 (±0.05) $\times 10^{-19}$ cm^3·molecules^{-1}·s^{-1} at 1 atm and 297 ± 1 K.

The gas-phase rate constant obtained in this study is >3 orders of magnitude smaller than those obtained by Hall et al.[25] and 1 order of magnitude smaller than that of Ariya et al.[18] We attribute these disagreements to different degrees and methods of consideration of the effect of surface-catalyzed and photoinduced reactions.

The effect of temperature on the reaction was studied. The second-order rate constants determined were 2.8 (±0.2) $\times 10^{-19}$ cm^3·molecule^{-1}·s^{-1} and 0.9 (±0.2) $\times 10^{-19}$ cm^3·molecule^{-1}·s^{-1} at 276 and 365 K, respectively. The rate constants decrease with an increase of the temperature between 276 and 365 K indicates an exothermic reaction. From the Arrhenius plot (Figure 5), the activation energy of the reaction of Hg^0 with Cl_2 was determined to be -1.2 (±0.2) $\times 10^4$ kJ·kmol^{-1} and the preexponential factor 1.8 (±0.2) $\times 10^{-21}$ cm^3·molecule^{-1}s^{-1}.

The Surface-Induced Reaction. As discussed and also from Table 2, we can see that the contribution from the reaction on the quartz window surface accounts for a substantial fraction in the overall Hg^0 decay rate. Its contribution increased with the decrease of the reactor volume. Also, we found that the quartz surface had a larger contribution when it was placed in the inflated part of the reactor than when placed in the neck. The former was about twice as large as the latter when $[Cl_2]$

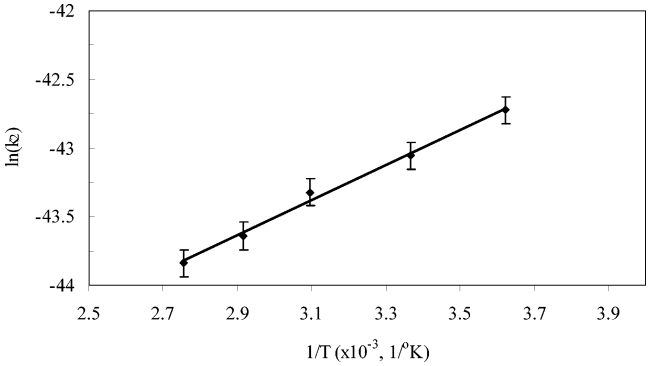

Figure 5. Relationship of $\ln(k_2)$ and $1/T$ at 760 Torr. The initial Hg^0 and Cl_2 concentrations were 4.4×10^{12} molecules·mL^{-1} and 6.5×10^{15} molecules·mL^{-1}, respectively. The reactors were coated with halocarbon wax.

was 6.5×10^{15} molecules·mL^{-1}. This indicates that a concentration gradient of Hg^0 was expected to develop across the neck section (along the length of the neck, L_f in Figure 1) as the reaction proceeded, because the quartz surface reaction rate was larger than the gas phase reaction rate. The mass transfer should take place only by the molecular diffusion in an enclosed and undisturbed system. The Hg^0 concentration in the bulk (the spherical bulge of the reactor) was assumed to be identical. The adsorption and reaction on the reactor wall were negligible because of the coating of the HW. According to a mass balance and diffusion-control-reaction theory,[26] the following equation can be obtained for the reaction rate on the quartz surface

$$A_q R_{sq} = A\frac{D}{L_f}([Hg^0] - [Hg^0]_s) = A_q k_{sq}'[Hg^0]_s = A_q \frac{1}{\frac{L_f}{D} + \frac{1}{k_{sq}'}}[Hg] \quad (7)$$

where R_{sq} (molecules·cm^{-2}·s^{-1}) is the reaction rate on quartz. L_f and A are the length of the neck and the surface area of quartz or the cross-section of the neck ($A = A_q$); D is the diffusion coefficient of Hg^0 in nitrogen, which can be estimated by the Satterfield model;[22] $[Hg^0]_s$ is the concentration of gas-phase Hg^0 adjacent to the surface; L_f/D and $1/k_{sq}'$ can be regarded as the diffusion resistance and reaction resistance, respectively;[24] and α_q in eq 2a was the local concentration distribution coefficient between the bulk gas and the quartz surface, which can be derived from eq 7 as

$$\alpha_q = \frac{[Hg^0]_s}{[Hg^0]} = \frac{1}{1 + \frac{k_{sq}'L_f}{D}} \quad (8)$$

It is obvious from eq 8 that α_q depends on both the diffusion rate and the reaction rate constant.

The rate constant of the reaction on the quartz surface, k_{sq}', can be determined from eq 7 and the data in Figure 4 as shown in Figure 6. It can be seen that k_{sq}' is linearly proportional to the concentration of chlorine. Therefore, the reaction kinetics on the quartz surface can be expressed as

$$R_{sq} = k_{sq}[Cl_2][Hg^0]_s \quad (9)$$

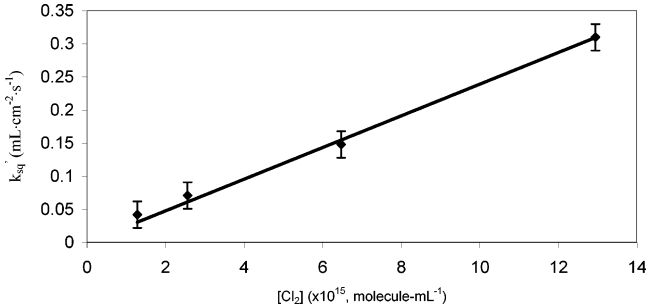

Figure 6. Rate constant of the reaction of Hg^0 with Cl_2 on the quartz surface as a function of the concentration of chlorine between 1.2×10^{15} molecule·mL^{-1} and 13×10^{15} molecule·mL^{-1}.

where k_{sq} is the second-order rate constant on the quartz surface; it was calculated to be 2.7×10^{-17} mL^2·molecules^{-1}·cm^{-2} ·s^{-1}. Here, the unit of gas concentration is in molecules/mL, instead of molecules/cm^3, to avoid canceling with the surface unit (in cm^2). The surface-induced reaction rate is proportional to the surface area.

The contribution of the gas-phase reaction to the overall reaction, k_g'/k_T, can be evaluated with eq 10, which was derived from eqs 6, 7, and 9 because the contribution of adsorption on the surface was small.

$$\frac{k_g'}{k_T} \approx \frac{k_3[M]}{\left(\frac{A_q}{V}\right)\left(\frac{1}{\frac{1}{k_{sq}} + \frac{[Cl_2]L_f}{D}} + k_3[M]\right)} \quad (10)$$

From eq 10, the effect of Cl_2 concentration, $[Cl_2]$, the volume of the reactor, V, and the diffusion coefficient, D, on k_g'/k_T can be predicted. Increasing the V and/or $[Cl_2]$ would increase the contribution of the gas-phase reaction, which would result in a decrease of the surface contribution (eq 4 and Table 1). The D will increase with a decrease of the gas pressure, causing a decrease of the Hg^0 diffusion resistance, L_f/D. As a result, the gas-phase reaction contribution would decrease (eq 10) and the surface-reaction contribution would increase (eqs 4 and 10 and Table 2).

Photoinduced Reaction. The pseudo-first-order overall rate constants, k_T, at various Cl_2 concentrations were determined under continuous and intermittent irradiations. Figure 7 shows that the overall rate constant, k_T, was larger when the reaction proceeded under a continuous irradiation (dotted line) than that under an intermittent irradiation (solid line) in the same reactor. The surface reaction was no longer dominant in the presence of the more rapid photoinduced reaction.

Similarly, by running experiments in three reactors, each component in k_T (eq 2a) can be calculated, given the fact that the gas-phase rate constant k_g' had been determined at the corresponding conditions. The results are summarized in Table 3. It can be seen that the apparent rate constant of the Hg^0 oxidation on the quartz surface, $\alpha_q k_{sq}'$, was almost the same as that of the oxidation without UV irradiation (shown in Table 1). The pseudo-first-order rate constant of the photoinduced gas reaction, k_p', was calculated to be 17.8×10^{-3} s^{-1} at 760 Torr and an intensity of 6.06×10^{16} photons·cm^{-2}·s^{-1}, which was about 16 times larger than that of the gas-phase reaction, k_g' (see Table 1), when $[Cl_2]$ was 6.5×10^{15} molecules·mL^{-1}.

Similar to the case of the gas-phase reaction, the photoinduced reaction rate appeared to be linearly

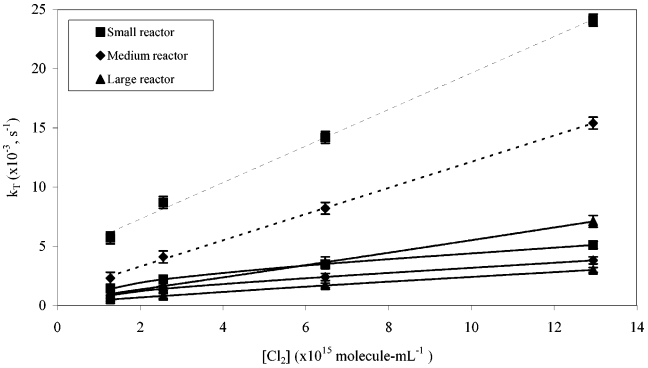

Figure 7. Effect of the 253.7 nm photon on the overall Hg^0 reaction rate constants with Cl_2 in three sizes of reactors. The Cl_2 concentrations studied were between 1.2×10^{15} molecule·mL^{-1} and 13×10^{15} molecules·mL^{-1}. Dotted lines indicate conditions with continuous UV irradiation at an intensity of 6.06×10^{16} photons·cm^{-2}·s^{-1}; solid lines indicate conditions with intermittent UV irradiation. All the reactors were coated with halocarbon wax.

Table 3. Effect of Gas Pressure on Photoinduced Pseudo-First-Order Rate Constant (k_p') and Surface Reaction on Quartz ($\alpha_q k_{sq}'$) at a Light Intensity of 6.06×10^{16} Photons·cm^{-2}·s^{-1} at 297 ± 1 K[a]

gas pressure (Torr)	k_p' ($\times 10^{-3}$ s^{-1})	$\alpha_q k_{sq}'$ ($\times 10^{-3}$ mL·cm^{-2}·s^{-1})
760	17.8 ± 0.5	53.4
264	6.4 ± 0.3	91.7

[a] $[Cl_2]$ at 6.5×10^{15} molecules·cm^{-3}.

dependent on the gas pressure (Figure 4), which suggests that the reaction is also a three-body collision process.

The use of mercury resonance absorption at 253.7 nm for the measurement of the Hg^0 concentration produces the $Hg^0(6^3P_1)$ excited state.[21] The radiative lifetime of the $Hg^0(6^3P_1)$ state in the transition to the $Hg^0(6^1S_0)$ ground state is 1.03×10^{-7} s.[27,28] However, the $Hg^0(6^3P_1)$ excited atoms can be quenched rapidly by a third body to produce the $Hg(6^3P_0)$ metastable state.[18] The quenching rate constant for this nonradiative transition is 7.1×10^{-12} mL·molecules^{-1}·s^{-1} at 1 atm N_2, which corresponds to the $Hg^0(6^3P_1)$ half-life of about 5×10^{-9} s. Consequently, the nonradiative transition from the $Hg^0(6^3P_1)$ state to the $Hg^0(6^3P_0)$ metastable state would be the dominant process under the experimental conditions employed. Since the radiative transition of $Hg^0(6^3P_0)$ to $Hg^0(6^1S_0)$ is doubly forbidden, the lifetime of the $Hg^0(6^3P_0)$ atoms are established by the quenching reactions. The quenching rate constant was determined to be 6.1×10^{-15} mL·molecules^{-1}·s^{-1}. Thus, the $Hg^0(6^3P_0)$ atoms possess a half-life of about 5×10^{-6} s at 1 atm N_2. Furthermore, the excited Hg_2 molecules can be produced in this system. The excited $Hg_2(^3l_u)$ molecules are formed in a triple collision of an $Hg^0(6^3P_0)$ atom, a ground-state $Hg^0(6^1S_0)$ atom, and an N_2 molecule.[29] The $Hg_2(^3l_u)$ molecule can then either decay spontaneously to the repulsive ground state with a decay constant comparable to that of the atomic 6^3P_1 resonance state, or it can collide with an N_2 molecule and be transferred to the metastable $Hg_2(^30^-_u)$ state, which has a radiative lifetime exceeding 4.5 ms. The aforementioned excited $Hg^0(6^3P_1$ and $6^3P_0)$ and $Hg_2(^3l_u$ and $^30^-_u)$ could react with the chlorine if the reactants are irradiated with 253.7 nm. The reaction rate constants of each excited Hg^0 and Hg_2 with chlorine are beyond the scope of this study.

The utilization efficiency of 253.7 nm photons for the oxidation of Hg^0, ϕ_{Hg}, can be approximately calculated according to eq 11, if the intensity of other wavelengths from the light source was small.[21]

$$\phi_{Hg} = \frac{\text{number of Hg}^0 \text{ molecules oxidized}}{\text{number of photons absorbed by Hg}^0} \quad (11)$$

Using the Beer−Lambert law[22] and a mercury absorption cross-section[25] of 4.5×10^{-16} cm^2·molecules^{-1}, the value of ϕ_{Hg} was calculated to be 6.7×10^{-4} molecules·photon^{-1} when $[Cl_2]$ was 6.5×10^{15} molecules·mL^{-1} at 1 atm. This result indicated that the utilization efficiency of 253.7 nm photons for the oxidation of Hg^0 is very small. Although the employed light source emits most of the intensity at 253.7 nm, it also emits photons at wavelengths between 320 nm and 440 nm, albeit at a much weaker intensity (<5% of that at 253.7 nm). However, Cl_2 dissociates to produce Cl atoms when it absorb[21,30] photons between 320 and 440 nm. The Cl atoms can react with Hg^0 rapidly. Consequently, the ϕ_{Hg} reported here should be considered as the upper limit of Hg^0 oxidation in terms of the utilization of 253.7 nm. Nevertheless, the lamp characteristic should not affect the determination of the gas-phase and surface-induced reaction rate constants, because both of them were determined in the dark as discussed before.

Conclusions

The oxidation of Hg^0 by Cl_2, as studied using a mercury photodetection technique, can occur by three concurrent reaction pathways: gas-phase, surface-induced, and photoinduced. The relative reaction rate of the gas-phase and surface-induced pathways was obtained by performing experiments using three reactors having different surface area-to-volume ratios. The photoinduced reaction rate was obtained by comparing experimental results between continuous and intermittent light illuminations. The pressure-dependent study revealed the reaction to proceed through a three-body collision process. The ternary gas-phase oxidation rate constant of Hg^0 by Cl_2 was determined to be 7.5 (±0.2) $\times 10^{-39}$ cm^6·molecules^{-2}·s^{-1} at 297 ± 1 K with N_2 the balance, which corresponds to a second-order rate constant of 1.82 (±0.05) $\times 10^{-19}$ cm^3·molecules^{-1}·s^{-1} at 1 atm N_2. The rate constant of the quartz surface-induced oxidation of Hg^0 by Cl_2 was 2.7×10^{-17} mL^2·molecules^{-1}·cm^{-2}·s^{-1}. The photoinduced oxidation of Hg^0 by Cl_2 accounts for a substantial fraction of Hg^0 oxidation under the experimental conditions employed; however, the utilization efficiency of the 253.7 nm photon for Hg^0 oxidation at $[Cl_2]$ of 6.5×10^{15} molecules·mL^{-1} was, at most, 6.7×10^{-4} molecules·photon^{-1}. The method developed here will be used for studying the fly ash or activated-carbon-catalyzed oxidation of Hg^0 molecules by gas oxidants under power plant flue gas conditions.

Acknowledgment

This work was supported by the Assistant Secretary for Fossil Energy, U.S. Department of Energy, under Contract DE-AC03-76SF0098 through the National Energy Technology Laboratory.

Literature Cited

(1) Wang, Q.; Shen, W.; Ma, Z. Estimation of Mercury Emission from Coal Combustion in China. *Environ. Sci. Technol.* **2000**, *34*, 2711.

(2) Sloss, L. L. Mercury—Emissions and Control. *The Clean Coal Centre Newsletter*; IEA Coal Research: London, U.K., 2002; No. 37, ISBN 92-9029-371-3.

(3) Senior, C. L.; Sarofim, A. F.; Zeng, T.; Helble, J.; Mamani-Paco, R. Gas-phase transformations of mercury in coal-fired power plants. *Fuel Process. Technol.* **2000**, *63*, 197.

(4) Galbreath, K. C.; Zygarlicke, C. J. Mercury Speciation in Coal Combustion and Gasification Flue Gases. *Environ. Sci. Technol.* **1996**, *30*, 2421.

(5) Krissmann, J.; Siddiqi, M. A.; Peters-Gerth, P.; Ripke, M.; Licas, K. A Study of the Thermodynamic Behavior of Mercury in a Wet Flue Gas Cleaning Process. *Ind. Eng. Chem. Res*. **1998**, *37*, 3288.

(6) Sliger, R. N.; Kramlich, J. C.; Marinov, N. M. Towards the Development of a Chemical Kinetic Model for the Homogeneous Oxidation of Mercury by Chlorine Species. *Fuel Process. Technol.* **2000**, *65*, 423.

(7) Senior, C. L. Behavior of Mercury in Air Pollution Control Devices on Coal-Fired Utility Boilers. Presented at Power Production in the 21st Century: Impacts of Fuel Quality and Operations, Engineering Foundation Conferences, Snowbird, UT, Oct 28−Nov 2, 2001.

(8) Givelet, N.; Roos-Barraclough, F.; Goodsite., M. E.; Cheburkin, A.; Shotyk, W. Atmospheric Mercury Accumulation Rates Between 5900 and 800 Calibrated Years BP in the High Arctic of Canada Recorded by Peat Hummocks. *Environ. Sci. Technol*. **2004**, *38*, 4964.

(9) Granite, E. J.; Pennline, H. W. Photochemical Removal of Mercury from Flue Gas. *Ind. Eng. Chem. Res.* **2002**, *41*, 5470.

(10) Blythe, G.; Richardson, C.; Rhudy, R. Pilot evaluation of the catalytic oxidation of mercury for enhanced removal in wet FGD systems. In *Proceedings of Air Quality III*, Proceedings of the Mercury, Trace Elements, and Particulate Matter Conference, Arlington, VA, Sept 9−12, 2002; Energy and Environmental Research Center, University of Dakota, Grand Fork, North Dakota, Sept 2002.

(11) Mendelsohn, M. H.; Livengood, C. D. Development of a Process for Combined Removal of Mercury and Nitrogen Oxides from Flue Gas. Presented at the 17th Annual International Pittsburgh Coal Conference, Pittsburgh, PA, Sept 11−14, 2000.

(12) Roy, S.; Rochelle, G. T. Chlorine Absorption in Sulphite Solutions: A Mechanism in Mercury Removal. Presented at A&WMA Mega Symposium and Specialty Conference on Mercury Emissions: Fate, Effects, and Control, Chicago, IL, Aug 20−23, 2001.

(13) Schroeder, W. H.; Yarwood, G.; Niki, H. Transformation processes involving mercury species in the atmosphere: Results from a literature survey. *Water, Air, Soil Pollut*. **1991**, *56*, 653.

(14) Seigneur, C.; Wrobel, J.; Constantinou, E. A Chemical Kinetic Mechanism for Atmospheric Mercury. *Envion. Sci. Technol*. **1994**, *28*, 1589.

(15) Hall, B. Ph.D. Dissertation, Chalmers University of Technology, University of Goteborg, Goteborg, Sweden, 1992.

(16) Schroeder, W. H.; Munthe, J. Atmospheric Mercury—An Overview. *Atmos. Environ.* **1998**, *32*, 809.

(17) Lin, C. J.; Pehkonen, S. O. The Chemistry of Atmospheric Mercury: A Review. *Atmos. Environ.* **1999**, *33*, 2067.

(18) Ariya, P. A.; Khalizov, A.; Gidas, A. Reaction of Gaseous Mercury with Atomic and Molecular Halogens. *J. Phys. Chem. A* **2002**, *106*, 7310.

(19) Edwards, J. R.; Srivastava, R. K.; Kilgroe, J. D. A study of gas-phase mercury speciation using detailed chemical kinetics. *J. Air Waste Manage. Assoc.* **2001**, *51*, 869.

(20) Widmer, N. C.; West, J.; Cole, J. A. Thermochemical study of mercury oxidation in utility boiler flue gases. Presented at the Air and Waste Management Association Annual Meeting, Salt Lake City, UT, June 18−22, 2000.

(21) Hall, B.; Schager, P.; Lindqvist, P. Experimental study on the rate of reaction between mercury vapour and gaseous nitrogen dioxide. *Water, Air, Soil Pollut*. **1995**, *81*, 121.

(22) Calvert, J. G.; Pitts, J. N.; *Photochemistry*; John Wiley & Sons, Inc.: New York, 1966.

(23) Benson, S. W. *The Foundations of Chemical Kinetics*; McGraw-Hill Book Co., Inc.: New York, 1960.

(24) Levenspiel, O. *Chemical Reaction Engineering*; John Wiley & Sons, Inc: New York, 1998.

(25) Hall, B.; Schager, P.; Lindqvist, P. Chemical reactions of mercury in combustion flue gases. *Water, Air, Soil Pollut*. **1991**, *56*, 3.

(26) Satterfield, C. *Mass Transfer in Heterogeneous Catalysis*; MIT press: Cambridge, MA, 1969.

(27) Tolman, R. Duration of Molecules in Upper Quantum States. *Phys. Rev*. **1924**, *23*, 693.

(28) Blagoev, K.; Bogdanovich, P.; Dimitrov, N.; Momkauskaite, A. Radiative Lifetime of $5d^{10}nl$ States of Hg^+. *Phys. Rev. A.* **1988**, *37*, 4679.

(29) Skonieczny, J.; Krause, L. Effect of Hg_2−Hg Collisions on the Formation and Decay of Excited Hg_2 Molecules in Hg−N_2 Mixtures. *Phys. Rev. A.* **1974**, *9*, 1612.

(30) Herzberg, G. *Molecular Spectra and Molecular Structure. I. Spectra of Diatomic Molecules*; D. Van Nostrand Co., Inc.: Toronto, Canada, 1967.

Received for review March 24, 2005
Revised manuscript received May 10, 2005
Accepted May 18, 2005

IE050377J